Supporting Information

How many tautomerisation pathways connect Watson-Crick-like G*·T DNA base mispair and wobble mismatches?

Ol'ha O. Brovarets' & Dmytro M. Hovorun✉

Department of Molecular and Quantum Biophysics, Institute of Molecular Biology and Genetics, National Academy of Sciences of Ukraine, 150 Akademika Zabolotnoho Str., 03680 Kyiv, Ukraine
Department of Molecular Biotechnology and Bioinformatics, Institute of High Technologies, Taras Shevchenko National University of Kyiv, 2-h Akademika Hlushkova Ave., 03022 Kyiv, Ukraine
✉Corresponding author. Email: dhovorun@imbg.org.ua

Table S1. Energetic characteristics of the investigated base mispairs and TSs of the conversion *via* the sequential obtained at the different levels of theory for the geometry calculated at the B3LYP/6-311++G(d,p) level of theory.

Complex	Level of theory							
	MP2/6-311++G(2df,pd)		**MP2/6-311++G(3df,2pd)**		**MP2/cc-pVTZ**		**MP2/cc-pVQZ**	
	ΔG^a	ΔE^b	ΔG^a	ΔE^b	ΔG^a	ΔE^b	ΔG^a	ΔE^b
G*·T(WC)	0.00	0.00	0.00	0.00	0.00	0.00	0.00	0.00
G·T*(WC)	1.16	1.14	1.27	1.24	1.40	1.38	1.22	1.19
G·T(w)	1.70	2.47	1.53	2.30	2.05	2.82	1.69	2.46
$TS_{G^*\cdot T(WC)\leftrightarrow G\cdot T^*(WC)}$	2.33	5.31	2.76	5.74	2.47	5.44	2.63	5.61
$G\cdot T(w_1)$	4.30	5.83	4.41	5.93	4.88	6.41	4.54	6.07
$G\cdot T(w_2)$	5.50	6.87	5.62	6.99	5.55	6.92	6.01	7.07
$TS_{G\cdot T(w_1)\leftrightarrow G\cdot T(w_2)}$	6.96	8.40	7.11	8.55	7.89	9.33	7.34	8.78
$TS_{G\cdot T(w_2)\leftrightarrow G\cdot T^{sym}(w_2)}$	12.24	12.89	12.51	13.16	12.28	12.94	12.58	13.23
G*·T*(w)	12.70	14.32	13.01	14.63	12.90	14.52	12.84	14.46
$TS^{G^+\cdot T^-}_{G\cdot T^*(WC)\leftrightarrow G^+\cdot T^-(w)}$	13.51	12.49	13.66	12.64	13.79	12.78	13.56	12.55
$TS_{G^+\cdot T^-(w)\leftrightarrow G^*\cdot T^*(w)}$	14.53	17.41	14.89	17.77	14.88	17.76	14.72	17.61
$G^+\cdot T^-(w)$	16.00	17.70	16.23	17.92	16.35	18.04	16.03	17.73
$TS^{G^+\cdot T^-}_{G\cdot T(w)\leftrightarrow G\cdot T^*(WC)}$	19.17	19.27	18.94	19.05	19.18	19.28	18.73	18.83
$TS^{G^-\cdot T^+}_{G\cdot T^*(WC)\leftrightarrow G\cdot T(w_1)}$	31.20	33.92	31.75	34.47	32.25	34.97	32.28	35.00
$TS^{G^-\cdot T^+}_{G^*\cdot T(WC)\leftrightarrow G\cdot T(w_2)}$	39.23	40.83	39.47	41.08	39.73	41.33	39.67	41.27

[a]The relative Gibbs free energy of the complex ($\Delta G_{G^*\cdot T(WC)}$=0; T=298.15 K), kcal·mol^{-1}

[b]The relative electronic energy of the complex ($\Delta E_{G^*\cdot T(WC)}$=0), kcal·mol^{-1}

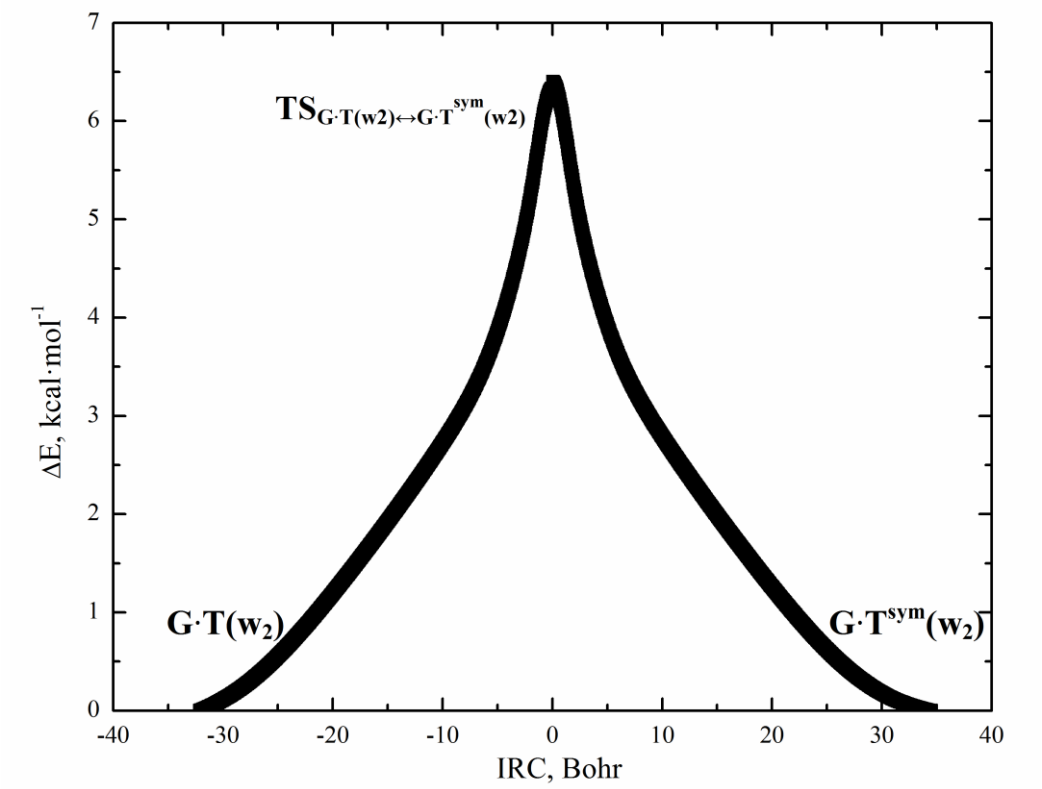

Fig. S1. Profile of the relative electronic energy ΔE of the G·T(w_2)↔G·T^{sym}(w_2) conformational interconversion of the mirror-symmetric enantiomers of the wobble G·T(w_2) base mispair *via* the rotation of the NH_2 amino group of the G base along the IRC obtained at the B3LYP/6-311++G(d,p) level of theory.

Table S2. Energetic and kinetic characteristics of the G·T(w_2)↔G·T^{sym}(w_2) conformational interconversion of the mirror-symmteric enantiomers of the wobble G·T(w_2) base mispair obtained at the different levels of theory for the geometry calculated at the B3LYP/6-311++G(d,p) level of theory.

Level of theory	$\Delta\Delta G_{TS}$[a]	$\Delta\Delta E_{TS}$[b]	$\tau_{99.9\%}$[c]
MP2/6-311++G(2df,pd)	6.73	6.01	$4.69\cdot10^{-8}$
MP2/6-311++G(3df,2pd)	6.89	6.17	$6.11\cdot10^{-8}$
MP2/cc-pVTZ	6.73	6.01	$4.68\cdot10^{-8}$
MP2/cc-pVQZ	6.89	6.17	$6.11\cdot10^{-8}$

[a]The Gibbs free energy barrier for the G·T(w_2)↔G·T^{sym}(w_2) conformational interconversion (T=298.15 K), kcal·mol^{-1}

[b]The electronic energy barrier for the G·T(w_2)↔G·T^{sym}(w_2) conformational interconversion, kcal·mol^{-1}

[c]The time necessary to reach 99.9% of the equilibrium concentration between the mirror-symmetric enantiomers, s

See also Table S1.

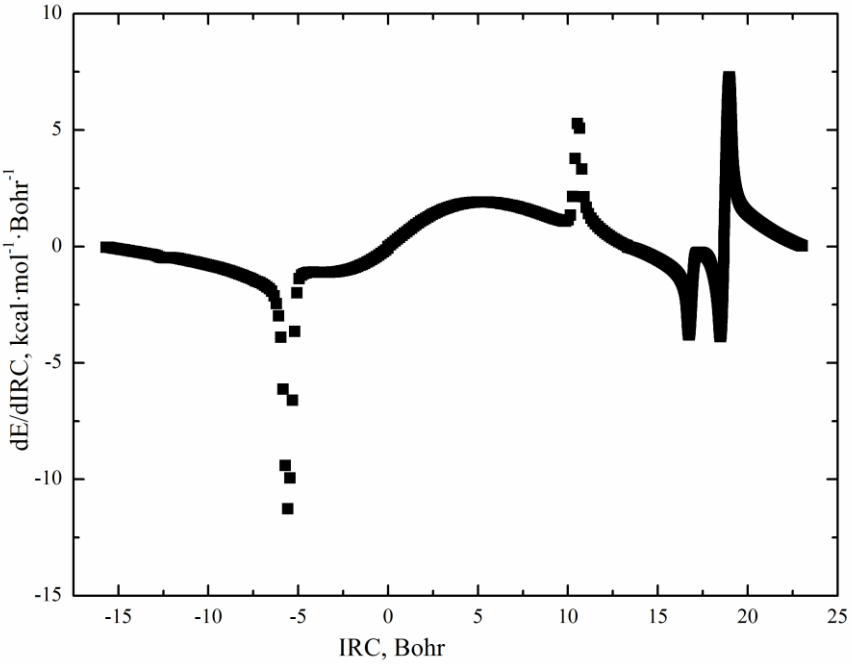

Fig. S2. Profile of the first derivative of the electronic energy with respect to the IRC (dE/dIRC) along the IRC of the G·T(w)↔G*·T(WC) tautomerisation *via* the sequential DPT obtained at the B3LYP/6-311++G(d,p) level of theory.

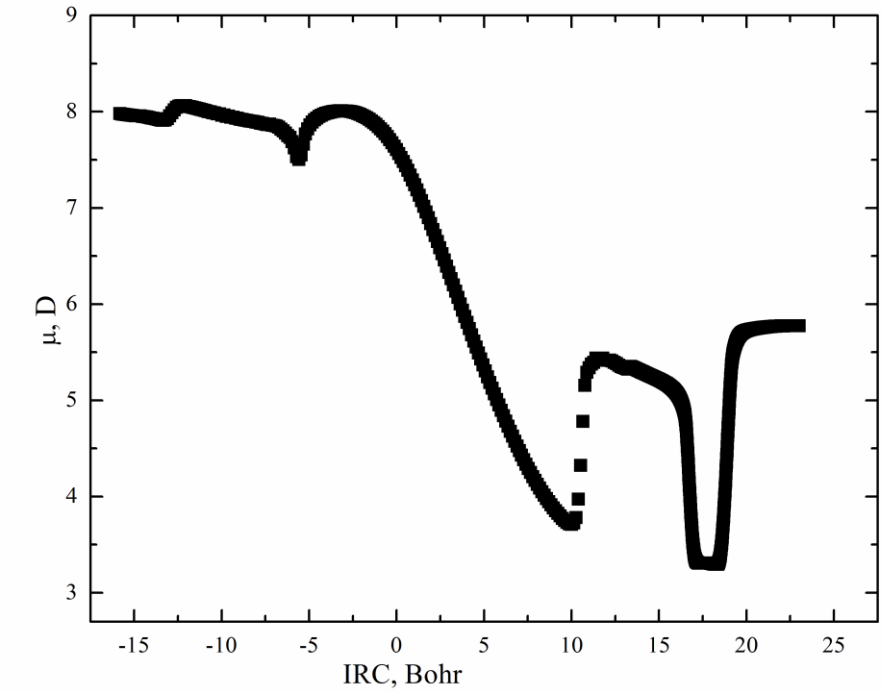

Fig. S3. Profile of the dipole moment μ of the base mispair along the IRC of the G·T(w)↔G*·T(WC) tautomerisation *via* the sequential DPT obtained at the B3LYP/6-311++G(d,p) level of theory.

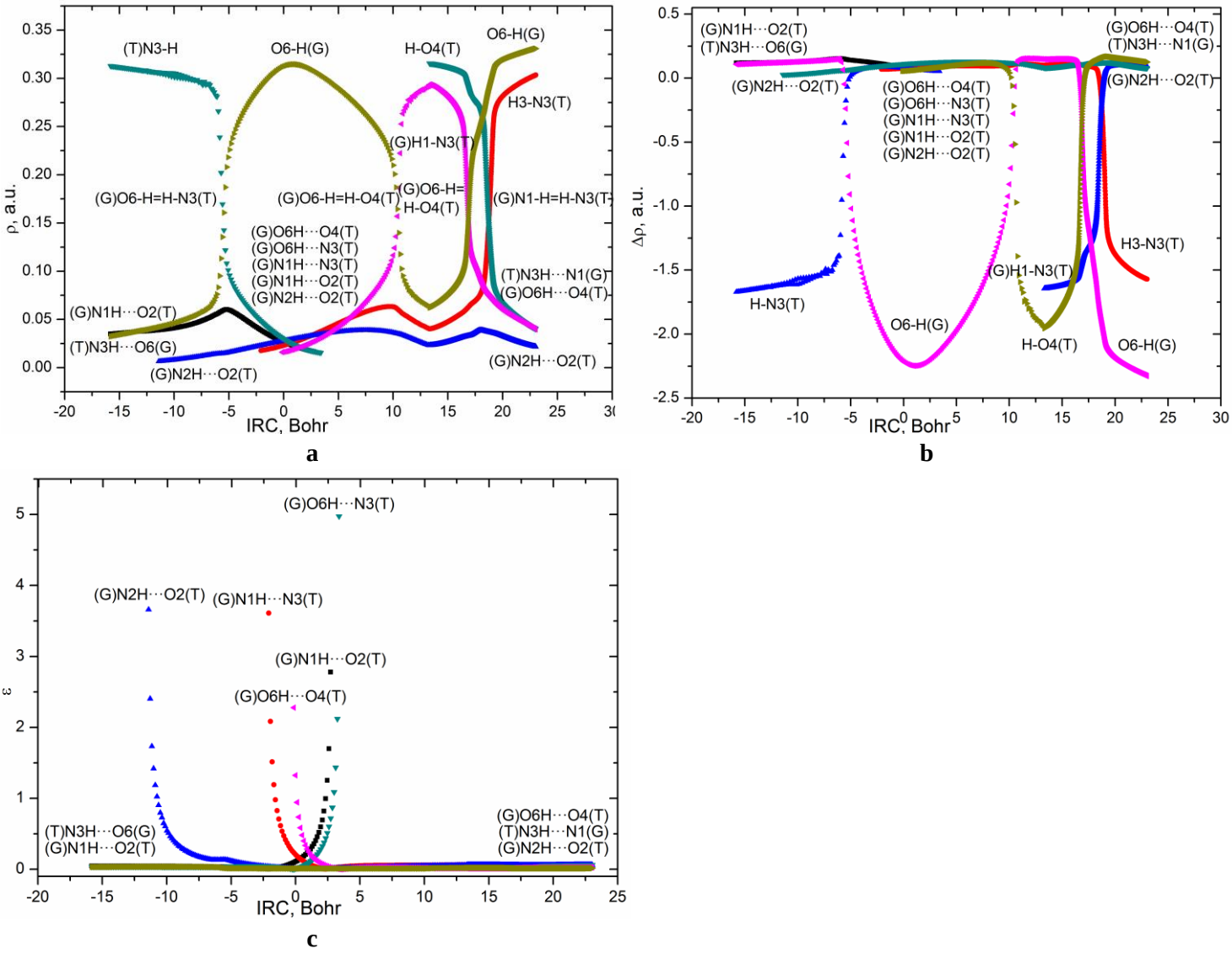

Fig. S4. Profiles of: (**a**) the electron density ρ; (**b**) the Laplacian of the electron density Δρ and (**c**) the ellipticity ε at the (3,-1) BCPs of the covalent and hydrogen bonds along the IRC of the G·T(w)↔G*·T(WC) tautomerisation *via* the sequential DPT obtained at the B3LYP/6-311++G(d,p) level of theory (see also Tables 1,7 and Figs. 7-9).

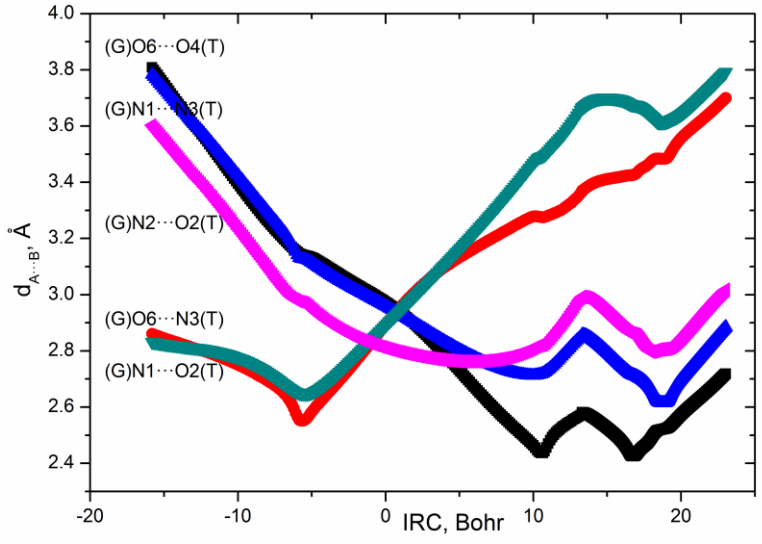

a

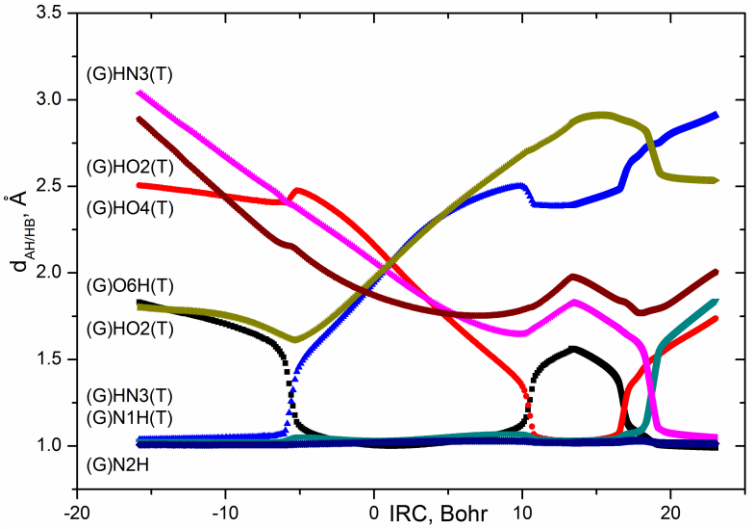

b

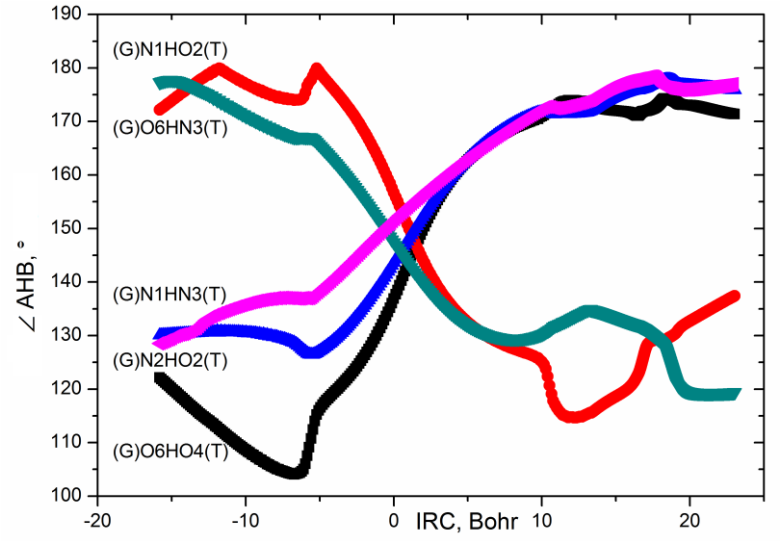

c

Fig. S5. Profiles of: (**a**) the distance $d_{A\cdots B}$ between the electronegative A and B atoms; (**b**) the distance $d_{AH/HB}$ between the hydrogen and electronegative A or B atoms and (**c**) the angle ∠AHB along the IRC of the G·T(w)↔G*·T(WC)) tautomerisation *via* the sequential DPT obtained at the B3LYP/6-311++G(d,p) level of theory (see also Figs. 7-9).